# TWO-PHASE PRESSURE DROPS FOR CANDU FUEL BUNDLES IN UNCREPT AND CREPT CHANNELS

### S.C. SUTRADHAR

Fuel Channel Thermalhydraulics Branch Chalk River Laboratories Chalk River, Ontario K0J 1J0 Canada

## **ABSTRACT**

Pressure-drop tests in Freon-134a were performed on aligned and misaligned 37-element CANDU® (C6) fuel bundles in uncrept and 3% crept channels. The results indicate that the two-phase pressure-drop profiles are similar in shape, but higher in magnitude, compared with the single-phase pressure-drop profiles. The two-phase multipliers (TPMs) are a strong function of the thermodynamic quality of the fluid. The measured TPMs of the bundles in the uncrept channel are higher than those in the crept channel. The measured TPMs for the aligned bundles agree well with the Beattie correlation.

## INTRODUCTION

Pressure tubes in ageing CANDU reactors undergo diametral expansion or creep. This increase in diameter affects the hydrodynamic characteristics of the fuel channel and, consequently, changes the pressure drop across the string of fuel bundles. The critical heat flux (CHF) of a bundle string and its pressure drop are the primary parameters that govern the calculation of critical channel power (CCP) of a reactor. An accurate prediction of the pressure drop across the fuel string is essential for the precise evaluation of CCP. When dryout occurs, a significant fraction of the channel is in boiling; therefore, knowledge of two-phase pressure drop for bundles in crept channels is important to determine accurately the CCP of ageing reactors.

In the CCP calculation, both single- and two-phase pressure drops need to be determined accurately because of the existence of both phases in reactor channels. A two-phase multiplier (TPM), defined as the ratio of two-phase to single-phase pressure-drop, is universally used in the pressure-drop calculation for reactor channels. Many forms of TPM prediction method, usually derived from tube databases, are currently available in the literature. Their application to CANDU bundles in uncrept and crept channels with two-phase flow needs to be examined to ensure reliable pressure-drop calculations.

No databases for two-phase pressure drop in crept channels are available for CANDU fuel bundles. Recently, a series of pressure-drop tests were performed at Chalk River Laboratories (CRL) for CANDU fuel bundles in both uncrept and 3% crept channels, using single- and two-phase refrigerant (Freon-134a) at reactor conditions. The pressure drop along the bundles was

<sup>®</sup> CANDU: CANada Deuterium Uranium; registered trademark of AECL.

measured using the retractable probe technique [1]. Bundle appendages contribute significantly to the overall channel pressure drop in both single- and two-phase flows. The probe measured the detailed axial pressure drop of the bundles, including their appendages, in uncrept and crept channels. The wall taps measured the pressure drop across misaligned bundle junctions. The pressure-drop data were analyzed and compared with the published TPM prediction methods.

## PREDICTION METHODS FOR TWO-PHASE MULTIPLIERS

Although several prediction methods for TPMs are available in the literature [2, 3], only a limited number of them are applicable to CANDU fuel bundles. Other pressure-drop studies at CRL suggest three methods for CANDU bundle geometry: the Beattie [4] and Friedel [5] correlations, and the homogeneous model [2].

### Beattie Correlation

The Beattie large-bubble TPM correlation is given by

$$\Phi_{o,B}^{2} = \left(1 + x \left(\frac{\rho_f}{\rho_g} - 1\right)\right)^{2-b} \left(\frac{\rho_{ip}}{\rho_f}\right)^{1-b} \left(\frac{\mu_{ip}}{\mu_f}\right)^{b} \tag{1}$$

where b is the exponent in the Blasius-type equation for single-phase friction factor (f=a Re<sup>-b</sup>), the value of b= 0.10583 is taken for CANDU bundles [6], x is the thermodynamic quality,  $\rho_g$  and  $\rho_f$  are the vapour and bulk fluid densities at saturation temperature, and  $\mu_f$  is the bulk fluid viscosity at saturation temperature. The two-phase density and viscosity are given as

$$\rho_{tp} = \rho_f (1 - \beta) + \rho_g \beta \tag{2}$$

$$\beta = \frac{x \rho_f}{x \rho_f + (1 - x)\rho_g} \tag{3}$$

$$\mu_{tp} = \mu_f \left( 1 + \frac{\left( 2.5 \mu_g + \mu_f \right) \beta}{\mu_g + \mu_f} \right) \tag{4}$$

## Friedel Correlation

The Friedel correlation for TPM is given by

$$\Phi_{o,F}^{2} = A + \frac{3.21x^{0.78} (1-x)^{0.224} \left[\frac{\rho_{f}}{\rho_{g}}\right]^{0.91} \left[\frac{\mu_{g}}{\mu_{f}}\right]^{0.19} \left[1 - \frac{\mu_{g}}{\mu_{f}}\right]^{0.7}}{Fr_{tp}^{0.0454} We_{tp}^{0.035}}$$
(5)

where

$$A = (1 - x)^2 + x^2 \left(\frac{\rho_f f_g}{\rho_g f_f}\right) \tag{6}$$

$$Fr_{tp} = \frac{G^2}{\rho_{tp}^2 gD}$$
 = Froude number (7)

$$We_{ip} = \frac{G^2 D}{\rho_{ip} \sigma}$$
 = Weber number (8)

$$\rho_{tp} = \left[\frac{x}{\rho_g} + \frac{(1-x)}{\rho_f}\right]^{-1} \tag{9}$$

Chen's correlation [7] is used for the liquid- and gas-phase friction factors, and the correlation is

$$f = 4 \left[ 3.48 - 1.7372 \ln \left[ \frac{2\varepsilon}{D} - \frac{16.2426}{\text{Re}} \ln \left[ \frac{(2\varepsilon/D)^{1.1098}}{6.0983} + \left( \frac{7.149}{\text{Re}} \right)^{0.8981} \right] \right]^{-2}$$
 (10)

In Equations 6 to 10, D is the hydraulic diameter, G is the mass flux,  $\sigma$  is the surface tension and  $\epsilon/D$  is the relative surface roughness of the bundle string; the friction factor, f, in Equation 10 is calculated for each phase depending on the Reynolds number, Re, of the corresponding phase. Suffixes f and g represent the liquid and gas phases, respectively.

# Homogeneous Model

The homogeneous model for TPM is

$$\Phi_{o,H}^{2} = \left[1 + x \left(\frac{\rho_{f}}{\rho_{g}} - 1\right)\right] \left[1 + x \left(\frac{\mu_{f}}{\mu_{g}} - 1\right)\right]^{-0.25}$$
(11)

Equation 11 is used for calculating TPM for the overall bundle. The effect of skin friction (a function of fluid viscosity) across an appendage is negligible, and the viscosity terms in the homogeneous model are dropped for TPM calculation for appendages. The modified homogeneous model for an appendage TPM is taken as:

$$\Phi_{o,H,m}^{2} = \left[1 + x \left(\frac{\rho_f}{\rho_g} - 1\right)\right] \tag{12}$$

## EXPERIMENTAL SET-UP AND FACILITY

Set-up and Facility.

The test section consists of a string of six unheated (simulated) CANDU bundles (Figure 1). The test section was placed inside horizontal fibreglass liners, one simulated the uncrept channel, and the other simulated the 3% uniformly crept channel, of a CANDU reactor. Two retractable probes were used in the test: one was located in an inner subchannel and the other in an intermediate subchannel of the string. The probes were made of 1.28-mm 304-stainless-steel hard-drawn tubing. Each tube had two pressure-sensing holes of 0.33-mm diameter that were diametrically opposite to each other. Bundle C (Figure 1) was used as the test bundle, and it could be rotated to create different degrees of misalignment at its upstream and downstream junctions.

# Aligned-bundle Test

The aligned bundle string, with the retractable probes, was installed in the liner. The required test conditions were set, first for the single-phase flow and then for the two-phase flow. The axial pressure drop was recorded at every 5-mm interval covering a distance of 725 mm (Figure 1).

## **Bundle Rotation Test**

The probes were removed for the rotation test. Bundle C was rotated at every  $2^{\circ}$  interval. The rotation covered a total angular misalignment from  $-12^{\circ}$  to  $210^{\circ}$  (covering at least 3 cycles of aligned-bundle configuration). DP-cells 1 and 2 measured the upstream and downstream junction pressure drops at selected test conditions.

## RESULTS AND DISCUSSIONS

# Aligned-bundle Tests

Figure 2 shows the typical single- and two-phase pressure-drop profiles measured along the aligned bundle string in the uncrept channel. The thermodynamic quality (x) for the two-phase flow corresponds to that at the middle of bundle C. The data for one (inner) probe is plotted in the figure, as both probes generated almost identical pressure-drop profiles. The figure shows that the single- and two-phase pressure drops are similar in shape; they differ only in magnitude. The pressure drop increases with increasing quality at the same mass-flow rate. Similarly, Figure 3 shows the pressure-drop profiles in the 3% crept channel. The overall pressure drop in the crept channel is lower than that in the uncrept channel. The TPMs for friction, bundle and appendages are calculated as the ratio of the measured two-phase to corresponding single-phase pressure drop. The measured TPM is determined as follows:

$$\Phi_o^2 = \frac{\Delta P_{tp}}{\Delta P_{sp}} \tag{13}$$

 $\Delta P_{tp} = \Delta P_{meas-tp} - \Delta P_{acc-tp}$   $\Delta P_{acc-tp} = \Delta P$  due to acceleration.  $\Delta P_{sp} = single-phase$  pressure drop

The acceleration pressure drop is calculated as follows [6]:

$$\Delta P_{acc-tp} = G^2 \Delta \left[ \frac{x^2}{\alpha \rho_g} + \frac{(1-x)^2}{(1-\alpha)\rho_f} \right]$$
(14)

The void fraction,  $\alpha$ , is given by [8]

$$\alpha = \frac{xv_g}{1.13(v_f + xv_{fg}) + \frac{j_g}{G}} \tag{15}$$

$$j_g = 1.41 \left( \frac{g \sigma v_f v_{fg}}{v_g} \right)^{0.25}$$
 (16)

In Equations 15 and 16,  $\nu$  is the specific volume. The overall bundle TPM includes a junction, the mid-plane spacers and bearing pads, two bearing-pad planes and one nominal bundle length for frictional loss. Figure 4 shows the aligned bundle TPMs (in black squares) as a function of quality in the uncrept channel, and the TPMs increase with increasing quality. Separate TPMs in uncrept and crept channels are obtained from the corresponding dataset for each channel type.

## **Bundle Rotation Tests**

The measured pressure drops, both single-and two-phase, across a junction are averaged over 180° junction rotation; the most-probable TPM is calculated using the average pressure-drop values. Figure 5 shows the single- and two-phase pressure-drop profiles across a junction as a function of junction rotation. Figure 4 shows the most-probable TPMs (in black diamonds) for the misaligned bundle string in the uncrept channel, and the junction misalignment has no effect on the bundle TPM (TPMs are the same for aligned and misaligned conditions).

# Comparison with Prediction Methods

Table 1 shows the measured TPMs for various components of the aligned bundle string. The measured TPMs are obtained using Equations 13 to 16 at corresponding flow conditions and for channel geometric (creep) variation. Table 2 shows the predicted TPMs for the different components of the aligned bundle string. Tables 1 and 2 show that the TPMs usually increase with quality and usually decrease with increasing channel creep. This is due to a significantly lower pressure drop in the crept channel than in the uncrept channel.

The measured and predicted (by different methods) TPMs are compared using the following error analysis.

Avg Error (%) = 
$$\frac{1}{n} \sum \frac{Pred. TPM - Meas. TPM}{Pred. TPM} \times 100$$
 (17)

RMS Error (%) = 
$$\frac{1}{n-1} \sqrt{\sum \left(\frac{Pred. TPM - Meas. TPM}{Meas. TPM}\right)^{2}} \times 100$$
 (18)

Table 3 compares the predicted TPMs for various components of the aligned bundle string. The homogeneous model significantly underpredicts the measured TPMs for all components of the string. All prediction methods significantly underpredict the TPM for the mid-plane spacers because a small pressure drop is measured across the spacers using a DP cell with a relatively high range. Figure 6 shows the comparison of the various prediction methods with the measured TPMs for the aligned bundle in uncrept channel at 15 kg/s mass-flow rate.

The errors between the measured and predicted TPMs for the Beattie and Friedel correlations are very close. However, the average error of the Friedel correlation is systematically higher than that of the Beattie correlation. The Beattie correlation, in its present form (as stated above), shows a good agreement with the measured bundle TPM, as compared to the other two methods. The systematic errors in the Friedel correlation may be improved using a correction factor, e.g., corrected for bundle geometry, as used in some thermalhydraulics computer codes.

### CONCLUSIONS

Pressure-drop data in Freon-134a were obtained for 37-element CANDU fuel bundles in uncrept and 3% crept channels. Both aligned and misaligned bundle tests were performed. The TPMs strongly depend on the thermodynamic quality of the fluid. Bundle TPMs in the uncrept channel are higher than those in the crept channel. Bundle misalignment, in general, has no effect on the TPMs. The measured TPMs for friction, bundle and appendages are compared with the available prediction methods. The Beattie correlation agrees well with the measured TPMs, whereas the Friedel correlation and the homogeneous model have large systematic biases in TPM prediction.

## **ACKNOWLEDGEMENTS**

The author wishes to acknowledge the funding by COG for this work. The author would also like to acknowledge the assistance of personnel in the Fuel Channel Thermalhydraulics Branch at CRL during the test and data analysis; and A. Hameed for the test in crept channel.

#### REFERENCES

- 1. Rummens, H.E.C., Dimmick, G.R. and Bindner, P.E., "Measurement of Axial Pressure Profiles for Nuclear Fuel Assemblies by using a Sliding Probe", Experimental Thermal and Fluid Sciences, 14:213-223, 1997.
- 2. Collier, J.G., "Convective Boiling and Condensation", 2<sup>nd</sup> Edition, McGraw-Hill Book Company, 1981.
- 3. Todreas, N.E. and Kazimi, M.S., "Nuclear Systems I: Elements of Thermal Hydraulic Design", Hemisphere Publishing Corporation, 1990.
- 4. Beattie, D.R.H., "Drag Reduction Phenomena in Gas-Liquid Systems", Proc. of the International Conference on Drag Reduction, September 4-6, Cambridge, England, Paper 3, 1974.
- 5. Friedel, L., "Improved Friction Pressure Drop Correlations for Horizontal and Vertical Two-Phase Pipe Flow", European Two-Phase Flow Group Meeting, Ispra, Italy, vol. 18, no. 7, pp. 485-492, 1979.
- 6. Snoek, C.W., "The Onset of Subcooled Nucleate Boiling in Nuclear Fuel Bundles", 7<sup>th</sup> Annual Conference of the Canadian Nuclear Society, Toronto, Ontario, 1986.
- 7. Chen, N.H., "An Explicit Equation for Friction Factor in Pipes", Ind. Eng. Chem. Fund., vol. 18, pp. 296-297, 1979.
- 8. Saha, P. and Zuber, N., "Point of Net Vapour Generation and Vapour Void Fraction in Subcooled Boiling", Proc. of 5<sup>th</sup> International Heat Transfer Conference, Tokyo, Paper B-4.7, 1974.

TABLE 1: MEASURED TPM FOR ALIGNED BUNDLE STRING

Channel	Mass-flow	Reynolds	Average	Average	TPMs (Measured)				
Creep	Rate	Number	Pressure	Quality	Friction	Midplane	Junction	Bundle	
(%)	(kg/s)	(-)	(kPa)	(%)					
0.0	14.98	272454	1812	1.30	1.2423	1.0970	1.1637	1.1916	
0.0	14.99	271726	1803	4.56	1.5208	1.7980	1.5199	1.5261	
0.0	15.01	271715	1799	6.78	1.7789	2.1434	1.7495	1.8032	
0.0	15.00	271177	1795	10.06	2.0174	3.1102	2.1996	2.1472	
0.0	15.03	270482	1783	15.85	2.3890	3.9763	2.9127	2.7149	
0.0	15.06	270301	1776	20.69	2.6016	4.9335	3.5665	3.1265	
0.0	20.99	360093	1650	3.04	1.6589	2.4411	1.4199	1.5727	
0.0	21.00	358991	1641	4.80	1.9157	3.1363	1.6615	1.8608	
0.0	20.99	357107	1627	6.76	2.1605	3.8241	2.0329	2.1738	
0.0	20.98	354772	1611	10.56	2.4561	5.0275	2.5584	2.6556	
0.0	20.99	352826	1594	14.53	2.7528	6.0473	3.2067	3.1407	
3.0	15.08	237036	1902	7.45	1.6849	2.5935	1.6487	1.7277	
3.0	15.09	233728	1834	14.01	2.2166	3.8059	2.3823	2.3623	
3.0	15.06	231510	1789	19.35	2.5121	5.1921	3.0242	2.8132	
3.0	15.10	230969	1761	22.31	2.9330	5.8153	3.3001	3.1701	
3.0	21.15	325402	1798	7.81	1.7384	2.6683	1.7838	1.9173	
3.0	21.17	320082	1721	11.70	2.0507	3.6451	2.3497	2.3480	

TABLE 2: PREDICTED TPM FOR ALIGNED BUNDLE STRING

Channel	Mass-flow	Reynolds	Average	Average	e TPMs (Predicted)			
Creep	Rate	Number	Pressure	Quality	Beattie Friedel		Homogeneous	
(%)	(kg/s)	(-)	(kPa)	(%)	(Bundle & Ap	pendages)	(Friction & Bundle)	Appendages
0.0	14.98	272454	1812	1.30	1.1443	1.2824	1.1030	1.1280
0.0	14.99	271726	1803	4.56	1.5052	1.7184	1.3524	1.4527
0.0	15.01	271715	1799	6.78	1.7481	1.9597	1.5138	1.6730
0.0	15.00	271177	1795	10.06	2.1059	2.2831	1.7425	1.9986
0.0	15.03	270482	1783	15.85	2.7428	2.8173	2.1296	2.5800
0.0	15.06	270301	1776	20.69	3.2764	3.2522	2.4375	3.0679
0.0	20.99	360093	1650	3.04	1.3797	1.5591	1.2702	1.3399
0.0	21.00	358991	1641	4.80	1.5987	1.7834	1.4201	1.5383
0.0	20.99	357107	1627	6.76	1.8453	2.0116	1.5841	1.7625
0.0	20.98	354772	1611	10.56	2.3210	2.4133	1.8875	2.1967
0.0	20.99	352826	1594	14.53	2.8220	2.8112	2.1921	2.6548
3.0	15.08	237036	1902	7.45	1.7624	1.9712	1.5005	1.6854
3.0	15.09	233728	1834	14.01	2.5047	2.6399	1.9525	2.3662
3.0	15.06	231510	1789	19.35	3.1563	3.1819	2.3233	2.9619
3.0	15.10	230969	1761	22.31	3.5510	3.5074	2.5420	3.3178
3.0	21.15	325402	1798	7.81	2.0278	2.0423	1.5734	1.7857
3.0	21.17	320082	1721	11.70	2.7077	2.5028	1.8930	2.2590

TABLE 3: COMPARISON OF TPM PREDICTION METHODS

		Errors								
		Beattie		Friede	el	Homogeneous				
		Average	RMS	Average	RMS	Average	RMS			
		(%)	(%)	(%)	(%)	(%)	(%)			
	Friction	6	16	11	15	-15	16			
	Midplane	-34	37	-30	34	-41	44			
	Aligned Junction	0	8	5	10	-12	14			
	Aligned Bundle	-1	9	4	9	-20	20			

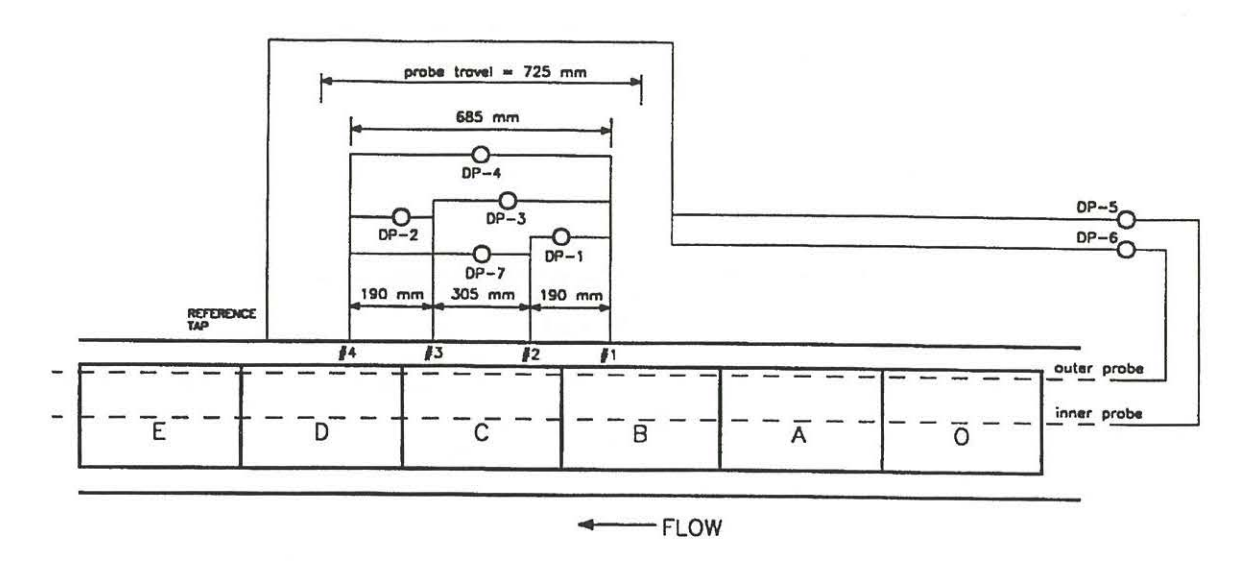


FIGURE 1: SCHEMATIC DIAGRAM OF TEST SECTION.

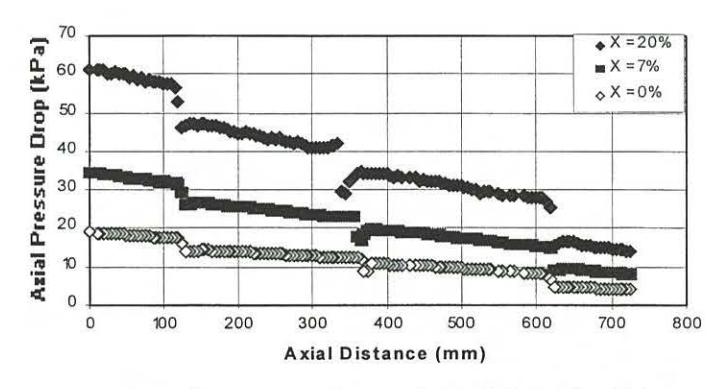


FIGURE 2: AXIAL PRESSURE-DROP PROFILES IN UNCREPT CHANNEL.

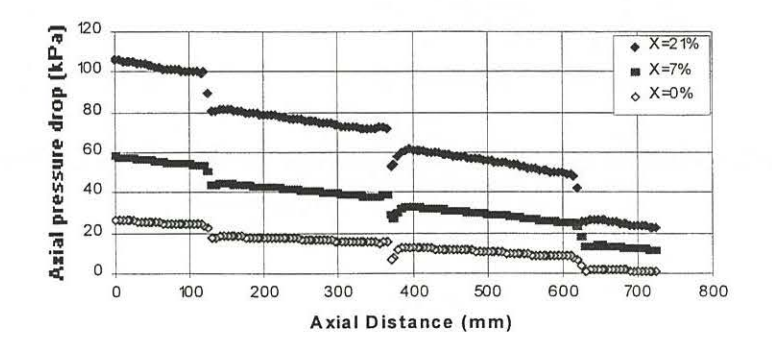


FIGURE 3: AXIAL PRESSURE-DROP PROFILES IN CREPT CHANNEL.

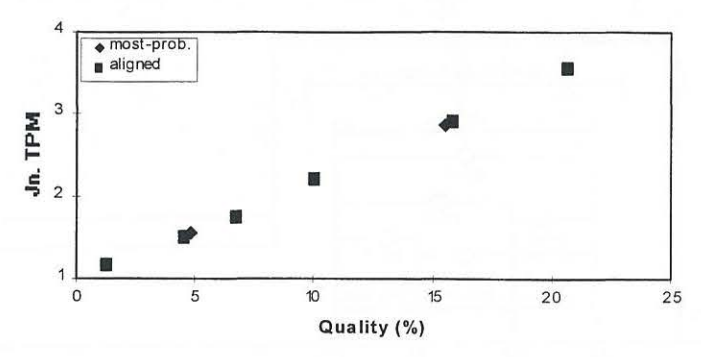


FIGURE 4: MOST-PROBABLE AND ALIGNED JUNCTION TPM IN UNCREPT CHANNEL.

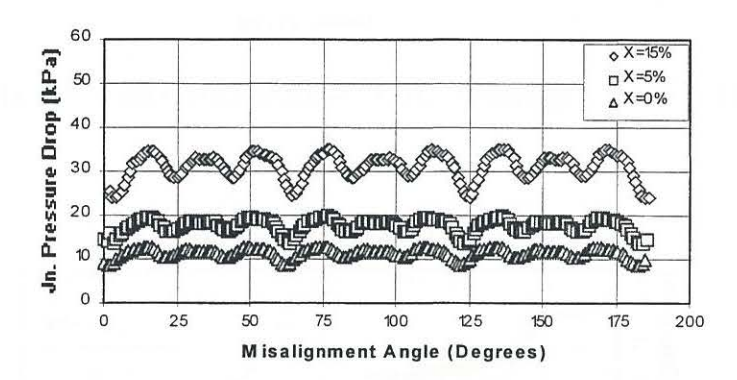


FIGURE 5: JUNCTION PRESSURE-DROP PROFILES IN UNCREPT CHANNEL.

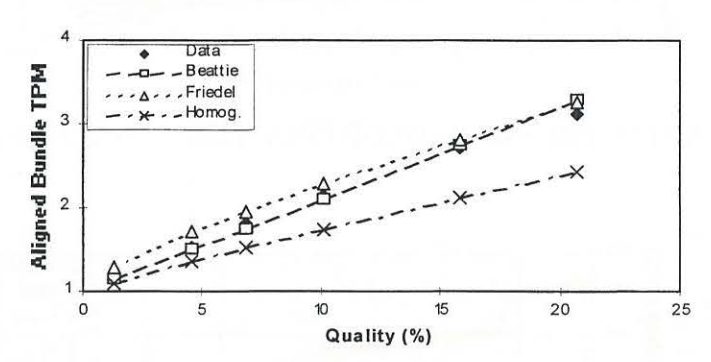


FIGURE 6: MEASURED TPM IN UNCREPT CHANNEL AND COMPARISON WITH PREDICTION METHODS.